Int. J. Heat Mass Transfer. Vol. 23, pp. 1686–1690

0017-9310/80/1201-1686 $02.00/0

MEASUREMENT AND PREDICTION OF THE PRESSURE DIFFERENCE THROUGH A TWO-PHASE LIQUID–METAL MHD GENERATOR

P. F. DUNN
Engineering Division, Argonne National Laboratory, Argonne, IL 60439, U.S.A.

(*Received* 29 *January* 1980 *and in revised form* 24 *April* 1980)

NOMENCLATURE

- a, electrode spacing;
- B, magnetic flux density (integral average);
- d_h, average hydraulic diameter, $2aw/(a+w)$
- l, distance between first and last pressure transducers;
- $\dot{m}_g$, mass flow rate of nitrogen;
- $\dot{m}_l$, mass flow rate of sodium;
- M, Hartmann number, $Bd_h\sqrt{(\sigma_l/\mu_l)}$;
- p, absolute pressure;
- R_i, internal resistance, $a/lw\sigma_l$(single-phase);
- R_{shunt}, liquid–metal shunt layer resistance, $a/2l\delta\sigma_l$;
- R_{wall}, conducting wall resistance, $a/2lt\sigma_{sst}$;
- Re, Reynolds number, $\rho_l u_l d_h/\mu_l$;
- t, conducting wall thickness;
- T, temperature;
- u_l, average liquid velocity, $\dot{m}_l/\rho_l aw$;
- w, average spacing between 'insulating' walls;
- α, average void fraction;
- δ, liquid–metal shunt layer thickness;
- Δp, pressure difference between first and last transducers;
- λ, resistance coefficient (friction factor), $(-\Delta p/l)(2d_h/\rho_l u_l^2)$;
- λ^*, normalized resistance coefficient, $\lambda_M - \lambda_{M=0}$;
- μ_l, absolute viscosity of liquid;
- ρ_l, density of liquid;
- σ_l, electrical conductivity of liquid;
- σ_{sst}, electrical conductivity of stainless steel;
- ϕ, conductivity ratio, $2t\sigma_{sst}/w\sigma_l$ (single-phase).

INTRODUCTION

THE EFFECTS of a magnetic field and other parameters on the pressure gradient through a liquid–metal magnetohydrodynamic (LMMHD) generator are examined in this study.

In 1978, data was gathered at Argonne National Laboratory (ANL), using the world's first high-temperature two-phase LMMHD generator. The primary objective of the tests that produced these data was to characterize the performance of the generator over the temperature range of approximately 500–800 K. During these experiments, the effects of temperature, applied magnetic field, and other parameters on the generator pressure gradient, electrode voltage, and gas-to-liquid velocity slip ratio were investigated. Some of the results are presented elsewhere [1, 2]. In this study, the pressure-gradient data for both single-phase (sodium) flow and two-phase (sodium–nitrogen) flow through the generator are reported and discussed.

A primary motivation for this and a companion study [3] was to develop a reliable method of predicting the total pressure difference through a two-phase LMMHD generator. Such power generators have been under development at ANL for a number of years. The references for these studies conducted at ANL and for the basic research studies on single-phase and two-phase flows that pertain to these generators were presented recently by Dunn [3]. The latest results of experiments on a LMMHD generator operated at ambient temperature were reported by Fabris *et al.* [4]. Branover *et al* [5] have developed an analytical model that considers the effects of a nonuniform void fraction distribution and, also, of a current-shunting liquid–metal layer on the performance of a two-phase LMMHD generator. Gershon and Lykoudis [6] have presented an analytical study concerning the effect of end-current losses on generator performance. The effect on generator performance of a difference in velocity between the gas and liquid–metal components of a two-phase mixture have been discussed by Fabris and Pierson [7].

THE EXPERIMENT

The subject experiments were conducted at the ANL two-phase sodium–nitrogen LMMHD facility, which is described elsewhere [8]. The liquid–metal MHD generator utilized for these tests is described in detail in [2]. Basically, it was a linear-tapered, rectangular, thin metal duct with 10.2-cm (4.0-in.) uniform electrode spacing and a variable 'insulating' wall spacing of 5.1 to 6.9 cm (2.0–2.7 in.) from its inlet to the outlet.

Thirty-seven system parameters—including temperatures, pressures, flow rates, voltages, magnetic flux densities, and void fractions—required for generator performance analysis, and 13 additional parameters required to monitor the system were measured, scanned, and stored by the facility data acquisition system for each experimental run. The duration of each run was approximately 15 min, during which each parameter was recorded a minimum of seven times. Each parameter varied by less than 2% from its average. The static pressures along the generator were measured with seven pressure transducers, which were spaced at intervals of approximately 10.5 cm (4.1 in.) along one generator electrode wall. The inlet gas pressure was monitored with an additional pressure transducer, and inlet liquid and gas temperatures with thermocouples located between the outer pipe walls and the piping insulation. Mass flow rates and mixture qualities were calculated from the volumetric flow rates measured by the respective liquid (electromagnetic) and gas flowmeters, the pressures, and the temperatures. A transverse magnetic field along 57 cm (22.25 in.) in the approximate center region of the generator was provided by an iron-core DC electromagnet, and the flux density was determined by means of the voltage drop across the calibrated current shunt. Voltages along the positive and negative electrodes were measured at five locations along each electrode. Thulium-170 gamma-ray sources were used in conjunction with detector/counter instrumentation to measure void fraction profiles at three locations along the length of the generator.

During the subject experiments, the generator operated at elevated temperatures for a total of 325 h, comprising nine

complete thermal cycles. The tests were made under open-circuit conditions, without the generator load resistors installed. A total of 14 single-phase (sodium) and 32 two-phase (sodium–nitrogen) tests were conducted over a range of sodium mass flow rates (14–28 kg s^{-1}), nitrogen mass flow rates (0–0.4 kg s^{-1}), average magnetic flux densities (0–0.9 T), and temperatures (490–735 K).

Standard estimates of error for the parameters measured were: sodium mass flow rate, 3.1%; nitrogen mass flow rate, 5.1%; temperature, 0.5%; pressure, 3.5%; magnetic flux density, 0.6%; wall voltage, 0.1%: and average void fraction, 13.8%.

PRESSURE MEASUREMENTS

Some of the static pressure measurements, taken at the seven positions along the length of the generator for various single-phase sodium mass flow rates and magnetic flux densities at 620 K are shown in Fig. 1(a). A moderate increase in the pressure along the length of the generator was measured for all cases in which no magnetic field was applied (case 1). Such an increase is the result of a decrease in the velocity along the length of the generator, which occurs because the cross-sectional area increases along the length. For all cases in which a magnetic field was applied (cases 2–5) a rise, followed by a decrease in pressure near the generator inlet was measured. Also, for these cases, a slight decrease, followed by a slight increase in pressure near the generator exit was noted. These entrance and exit changes in the pressure gradient are the result of circulating end currents in the liquid-metal, which increase the generation of power near the inlet of the generator and decrease it near the exit.

Figure 1(b) shows the measured static pressures along the length of the generator for various two-phase flow cases at 540 K in which the nitrogen mass flow rate was constant and the sodium mass flow rate and magnetic flux density varied. For the cases of lower magnetic flux density (cases 2 and 5), the pressure difference through the generator was relatively small. For cases of higher magnetic flux density (cases 3 and 4), the pressure difference was larger (Δp = 0.73 MPa for case 3 and 0.86 MPa for case 4). However, these pressure differences are still relatively small when compared with those measured in a LMMHD generator for the same mass flow rates and magnetic flux densities, but with an external electrical load connected to the generator electrodes [4]. For cases in which the sodium mass flow rate, magnetic flux density, and temperature were constant, the generator pressure difference was found to increase with an increase in the average void fraction of the two-phase mixture flow through the generator.

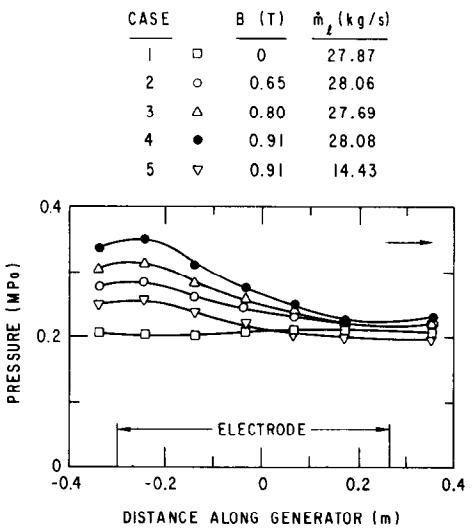

FIG. 1(a). Single-phase sodium pressure data, $T \cong$ 620 K.

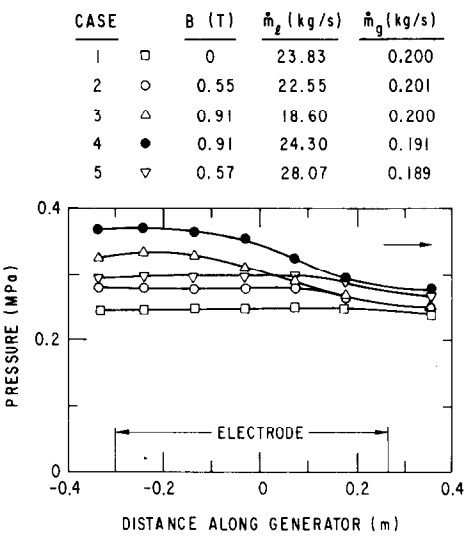

FIG. 1(b). Two-phase sodium–nitrogen pressure data, $T \cong$ 540 K.

ANALYSIS

At present, a derivation of an analytical expression for the pressure gradient through a two-phase LMMHD generator in a rigorous manner from the governing hydrodynamic equations appears intractable. In the past, however, several studies modeling two-phase LMMHD flows, principally those of Thome [9], Tanatugu *et al.* [10]. Serizawa and Michiyoshi [11], and Owen *et al.* [12], have adopted a more simplistic, yet effective analytical approach. The two-phase mixture was considered to be homogeneous with respect to its density, viscosity, electrical conductivity, and velocity. This approach leads to the desired expression for the two-phase case written in terms of single-phase quantities and the average void fraction of the mixture.

Recent studies at ANL also have demonstrated this approach to be quite successful in modeling the two-phase MHD pressure difference through a circular pipe with conducting walls [3, 13] and through a LMMHD generator operated with an electrical load [13, 14]. In the subject study, this model is extended to consider two-phase flow at high Hartmann numbers through a LMMHD generator with very thin conducting walls between the electrodes that is operated under open-circuit conditions.

Following this approach, the MHD contribution to the two-phase pressure difference is represented in nondimensional terms by the two-phase normalized resistance coefficient (friction factor), which is defined by the expression:

$$\lambda^*_{TP} \equiv \lambda_{TP,M} - \lambda_{TP,M=0} = \left\{\left(\frac{-\Delta p}{l}\right)_{TP} \cdot \frac{2d_h}{\rho_{TP} u^2_{TP}}\right\}_M - \left\{\left(\frac{-\Delta p}{l}\right)_{TP} \cdot \frac{2d_h}{\rho_{TP} u^2_{TP}}\right\}_{M=0}. \quad (1)$$

In the above expression, d_h is the average hydraulic diameter of the channel, and u_{TP} and ρ_{TP} the liquid velocity and density of the two-phase mixture, in that order. The two-phase pressure gradient was approximated in the above expression by $(-\Delta p/l)_{TP}$, where Δp is the pressure difference between the generator's first and last pressure transducers and l the distance between them. For a rectangular generator

geometry and high Hartmann numbers ($M \gg 1$), the two-phase normalized resistance coefficient can be related to the two-phase Hartmann number, M_{TP}, Reynolds number, Re_{TP}, and conductivity ratio, ϕ_{TP}, by the expression:

$$\lambda^*_{TP} = \frac{2M_{TP}}{Re_{TP}}\left\{\frac{M_{TP}\phi_{TP}+1}{1+\phi_{TP}}\right\}. \quad (2)$$

The derivation of the dimensional form of this expression for the single-phase case was presented by Thome [9], and the equivalent expression for the two-phase case by Owen *et al.* [12].

Expressions for the two-phase Hartmann and Reynolds numbers can be developed in terms of single-phase quantities and the average void fraction by defining the liquid velocity, electrical conductivity, density, and viscosity of the two-phase mixture, in that order, as:

$$u_{TP} = u_l/(1-\alpha), \quad (3)$$

$$\sigma_{TP} \equiv \sigma_l \cdot \exp(-3.8\alpha), \quad (4)$$

$$\rho_{TP} \equiv \rho_l \cdot f(\alpha), \quad (5)$$

and

$$\mu_{TP} \equiv \mu_l \cdot g(\alpha). \quad (6)$$

In these expressions, α denotes the average void fraction, and $f(\alpha)$ and $g(\alpha)$ unprescribed functions of α. Expression (4) is an empirical formula for the two-phase electrical conductivity proposed by Petrick and Lee [15], which best-fits the two-phase conductivity in LMMHD generators over the approximate void fraction range of 0.3–0.7. Expression (3) is derived from conservation of mass. Using these equations, the two-phase equivalents of the Hartmann and Reynolds numbers become:

$$M_{TP} \equiv Bd_h\sqrt{(\sigma_{TP}/\mu_{TP})} = M \cdot \sqrt{[1/g(\alpha)]} \cdot \exp(-1.9\alpha), \quad (7)$$

and

$$Re_{TP} \equiv \rho_{TP}\mu_{TP}d_h/\mu_{TP} = Re \cdot f(\alpha)/[(1-\alpha)\cdot g(\alpha)], \quad (8)$$

where M and Re represent the Hartmann and Reynolds numbers for the pure-liquid case.

The two-phase equivalent of the conductivity ratio can be defined as the ratio of the internal and external two-phase resistances of the generator. For the open-circuit case, the electrical load resistance of the generator is infinite, and the electrical end resistance is assumed to be large compared with the electrical shunt and wall resistances. The two-phase internal resistance is the two-phase core resistance, where

$$R_{i,TP} = a/lw\sigma_{TP} = a/lw\sigma_l \exp(-3.8\alpha), \quad (9)$$

in which a is the electrode spacing and w the average channel width in the direction parallel to B. The external resistance is the parallel combination of the resistance of the conducting walls between the electrodes,

$$R_{\text{wall}} = a/2lt\sigma_{sst}, \quad (10)$$

and the resistance of the liquid–metal shunt layer adjacent to the walls that are perpendicular to the electrodes,

$$R_{\text{shunt}} = a/2l\delta\sigma_l, \quad (11)$$

where σ_{sst} is the electrical conductivity of the stainless steel, t the conducting wall thickness, and δ the liquid–metal shunt layer thickness. The shunt layer thickness has been shown by Lykoudis [16] to be approximated by the expression:

$$\delta \cong \frac{w}{2}M^{-2/3} \quad (12)$$

for the case of a two-phase LMMHD generator operated under open-circuit conditions. Using equations (8)–(12), the expression for the two-phase conductivity ratio becomes:

$$\phi_{TP} = \left(\frac{2t\sigma_{sst}}{w\sigma_l} + M^{-2/3}\right)\exp(3.8\alpha). \quad (13)$$

The term, $2t\sigma_{sst}/w\sigma_l$, is the conductivity ratio for the single-phase case, which is denoted as ϕ. Note that for very large M the contribution of the shunt layer is negligible.

The expression for the two-phase normalized resistance coefficient, equation (1), can be recast solely in terms of measured quantities to become:

$$\lambda^*_{TP} = \left[\left\{\left(\frac{-\Delta p}{l}\right)_{TP}\cdot\frac{2d_h}{\rho_l u_l^2}\right\}_M - \left\{\left(\frac{-\Delta p}{l}\right)_{TP}\cdot\frac{2d_h}{\rho_l u_l^2}\right\}_{M=0}\right]\frac{(1-\alpha)^2}{f(\alpha)}. \quad (14)$$

Equation (2) can be rewritten as:

$$\lambda^*_{TP} = \frac{2M}{Re}\left\{\frac{M^{1/3}+M\phi+\sqrt{[g(\alpha)]}\exp(-1.9\alpha)}{M^{-2/3}+\phi+\exp(-3.8\alpha)}\right\} \times\left(\frac{1-\alpha}{f(\alpha)}\right)\exp(-3.8\alpha). \quad (15)$$

For all of the two-phase cases examined, values of the product $\sqrt{[g(\alpha)]}\cdot\exp(-1.9\alpha)$ were much less than $M^{1/3}$ or $M\phi$, where exact expressions for $g(\alpha)$ given by Wallis [17] and by Tanatugu *et al.* [10] were tested. Equation (15) reduces to:

$$\lambda^*_{TP} = \frac{2M^2}{Re}\left\{\frac{M^{-2/3}+\phi}{M^{-2/3}+\phi+\exp(-3.8\alpha)}\right\} \times\left(\frac{1-\alpha}{f(\alpha)}\right)\exp(-3.8\alpha). \quad (16)$$

The two-phase normalized resistance coefficients of the measured pressure differences computed by using equation (14) are compared in Fig. 2 with the predictions computed by using equation (16). For simplicity, $f(\alpha)$ was assumed equal to one in equations (14) and (16) because its exact expression does not affect the comparison between experimental and theoretical values. However, it is important to note that an exact expression for $f(\alpha)$ must be specified when using equation (16) to compute the magnitude of λ^*_{TP}. The linear least-squares fit of the data agreed with predicted values to within 20% (correlation coefficient = 0.85, standard error of estimate = 0.09).

DISCUSSIONS AND CONCLUSIONS

In the foregoing analysis several approximations were made in order to model the experimental results. Because the complete angle of divergence between the 'insulating' walls of the generator was small (equal to 0.0314 rad), the cross-sectional area of the generator was assumed constant and equal to the product of the electrode spacing, a, and the average spacing between the 'insulating' walls, w. The hydraulic diameter of the generator was computed by using the average spacing, w. The magnetic flux density was determined from an integral average of the flux density profile and the measured centerline flux density. The void fraction measured at the center location along the axis of the generator was chosen to represent the average void fraction of the two-phase mixture inside the duct of the generator.

The MHD pressure gradient for two-phase flow was approximated by the use of a normalized pressure difference based upon the difference between absolute pressures measured at the first and last pressure transducers located just beyond each end of the generator electrodes. This assumption

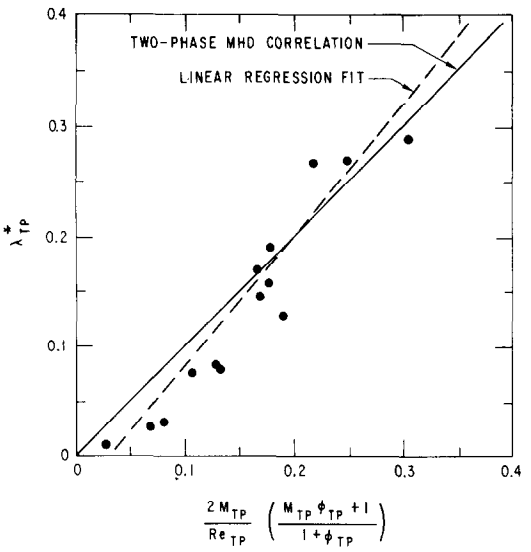

FIG. 2. Two-phase normalized resistance coefficient, measurements vs theory, $500\,K \lesssim T \lesssim 675\,K$.

is justifiable if magnetic-field entrance and exit effects are not large. Unfortunately, the conditions under which magnetic-field entrance and exit effects are sufficient to alter the two-phase MHD pressure gradient for the case of a rectangular geometry have not been specified, mainly because measured profiles of the pressure along the flow direction, before, within, and beyond the magnetic-field region have not been reported. In the case of pure liquid–metal MHD flows, measurements have been reported by Branover [18], for a rectangular channel with 'insulating' walls, and by Fabris *et al.* [4], for a rectangular MHD generator with an expanding cross-sectional area. Recently, measurements made for both single-phase and two-phase MHD flows through a pipe with weakly conducting walls were presented by Dunn [3]. All three of these investigations support the thesis that magnetic-field entrance and exit effects predominate in cases of high magnetic interaction, when single-phase magnetic interaction parameter (M^2/Re) values are on the order of 100 or larger. In the subject investigation, all cases examined had single-phase magnetic interaction parameter values of less than 100.

The single-phase Reynolds number for these experiments ranged from 5.8×10^5 to 1.1×10^6; the single-phase Hartmann numbers ranged from 3.0×10^3 to 7.9×10^3, and were equal to zero in some cases. In 8 of the 10 single-phase cases examined, in which the Hartmann number was greater than zero, it was sufficient to 'laminarize' the flow, according to the criterion for transition from turbulent to 'laminarized' flow discussed by Branover [18].

Equation (12) is an approximation for the shunt layer thickness and is applicable to limiting cases in which $\phi \ll 1$. For larger values of ϕ, the exponent of the Hartmann number in the equation changes and approaches a value of $-4/3$ for limiting cases in which $\phi \gg 1$, as was shown by Lykoudis [16].

Values of the two-phase normalized resistance coefficients predicted by the subject method are dependent upon the expressions chosen for the two-phase equivalents of the electrical conductivity, density, and absolute viscosity. In this investigation, the experimental conditions were such that the comparison between experimental and predicted values of the normalized resistance coefficient was dependent only upon the two-phase conductivity expression. The expression for the two-phase conductivity proposed by Petrick and Lee [15] was chosen because of its agreement with measurements in two-phase LMMHD generators over a wide void-fraction range [19]. An alternative expression could have been chosen.

It is concluded that the present model, which considers the effect of the liquid–metal shunt layer, can predict, to within experimental error, the total pressure difference through a two-phase LMMHD generator operated at high Hartmann numbers under open-circuit conditions.

Acknowledgements—This research was supported jointly by the U.S. Department of Energy and the Office of Naval Research. The experimental facility was constructed in part with funds from the Office of Naval Research and the National Science Foundation. I also acknowledge Prof. P. S. Lykoudis and Dr. E. S. Pierson for their technical advice and comments, and J. D. Staffon, P. V. Dauzvardis and R. A. Vallrugo for their able assistance in conducting the experiments.

REFERENCES

1. P. F. Dunn, E. S. Pierson, J. D. Staffon, P. V. Dauzvardis and I. Pollack, High-temperature liquid–metal MHD generator experiments, in *18th Symp. Engng Aspects of MHD*, D-2.2.7–D-2.2.12. Butte, MT (1979).
2. M. Petrick, P. F. Dunn, P. S. Lykoudis, E. S. Pierson, D. Cohen, F. Schreiner, P. V. Dauzvardis and I. Pollack, Liquid–metal MHD energy conversion, Argonne National Laboratory Report ANL/MHD-79-2 (1979).
3. P. F. Dunn, Single-phase and two-phase magnetohydrodynamic pipe flow, *Int. J. Heat Mass Transfer* **23**, 373–385 (1980).
4. G. Fabris, E. S. Pierson, I. Pollack, P. V. Dauzvardis and W. Ellis, High-power-density liquid–metal MHD generator results, in *18th Symp. Engng Aspects of MHD*, D-2.2.1–D-2.2.6. Butte, MT (1979).
5. H. Branover, A. Yakhot and A. El-boher, Hydrodynamic investigation of single-phase and two-phase flow in liquid–metal MHD-generator channels, April 1978 to March 1979 Annual Report No. ME 5-79, Department of Mechanical Engineering, Ben-Gurion University of the Negev, Israel (1979).
6. P. Gershon and P. S. Lykoudis, Analytical study of end effects in liquid–metal MHD generators, Final Report, Magneto-Fluid-Mechanics Laboratory, Purdue University (1978).
7. G. Fabris and E. S. Pierson, The role of interfacial heat and mechanical energy transfers in a liquid–metal MHD generator, *Energy Conversion* **19**, 111–118 (1978).
8. P. F. Dunn, High-temperature liquid-metal MHD facility, system design description, Engineering Division Document No. G0017-0157-SA-01, Argonne National Laboratory (1977).
9. R. J. Thome, Effect of a transverse magnetic field on vertical two-phase flow through a rectangular channel, Argonne National Laboratory Report ANL-6854 (1964).
10. N. Tanatugu, Y. Fujii-e and T. Siuta, Frictional pressure drop for Nak–N_2 two-phase flow in a rectangular cross-section channel of large aspect ratio, *J. Nucl. Sci. Technol.* **10**, 219–226 (1973).
11. A. Serizawa and I. Michiyoshi, Void fraction and pressure drop in liquid–metal two-phase flow, *J. Nucl. Sci. Technol.* **10**, 435–445 (1973).
12. R. G. Owen, J. C. R. Hunt and J. G. Collier, Magnetohydrodynamic pressure drop induced two-phase flow, *Int. J. Multiphase Flow* **3**, 23–33 (1976).
pressure-gradient correlations, in *MHD Flows and Turbulence—II*, pp. 145–156. Israel Universities Press, Israel (1980).
13. P. F. Dunn, G. Fabris, E. S. Pierson and M. Petrick, Two-phase liquid-metal MHD generator experiments and pressure-gradient correlations, 2nd Conference on

MHD-Flows and Turbulence, Bat-Sheva, Israel (1978).
14. M. Petrick, P. F. Dunn, E. S. Pierson, P. V. Dauzvardis and I. Pollack, liquid-metal MHD energy conversion, March 1976 to September 1977 Status Report, Argonne National Laboratory Report, ANL/MHD 78-5 (1978).
15. M. Petrick and K. Y. Lee, Performance characteristics of liquid-metal MHD generator, in *Proc. Symp. on MHD Elec. Power Gen.*, Vol. 2, pp. 953–970 (1964).
16. P. S. Lykoudis, Shunt-layer thickness, Argonne National Laboratory LMMHD Group Memo 77-2 (1977).
17. G. B. Wallis, *One-Dimensional Two-Phase Flow*. McGraw-Hill, New York (1969).
18. H. Branover, *Magnetohydrodynamic Flow in Ducts*. Wiley, New York (1969).
19. M. Petrick, Two-phase flow liquid-metal MHD generator, in *MHD Flows and Turbulence*, pp. 125–245. Wiley, New York (1976).

Int. J. Heat Mass Transfer. Vol. 23, pp. 1690–1693
Pergamon Press Ltd. 1980. Printed in Great Britain

A NOTE ON MASS TRANSFER IN TURBULENT WALL JETS

V. KUPPU RAO
Department of Mechanical Engineering, Indian Institute of Science, Bangalore 560012, India

(*Received* 20 *August* 1979 *and in revised form* 1 *April* 1980)

NOMENCLATURE

a, exponent;
A, constant;
b, exponent;
B, constant;
c, mass concentration;
c_0, mass concentration at the surface of the porous plate;
d_0, width of nozzle (PWJ); diameter of nozzle (RWJ);
E, constant;
F, non-dimensional stream function;
G, non-dimensional concentration;
K, exchange coefficient;
u, mean velocity in the direction of flow;
U_M, maximum velocity (wall Jet);
U_0, nozzle exit velocity;
v, mean velocity in the transverse direction;
x, longitudinal coordinate;
x_0, distance of leading edge of porous plate from the virtual origin;
y, transverse coordinate;
y_n, height of nozzle above flat plate—radial wall jet;
δ, boundary layer thickness (for wall jets δ is the height at which $u = U_M/2$);
δ_c, concentration boundary layer thickness;
δ_M, height at which $u = U_M$;
η, similarity parameter (y/δ);
η_M, value of η at which $u = U_M$;
ζ, similarity parameter (y/δ_c);
u', v', c', turbulent fluctuations in u, v and c;
ρ, density;
ν, kinematic viscosity;
τ_0, wall shear stress;
τ, shear stress;
ε_M, diffusivity of momentum (turbulent);
ε_m, diffusivity of mass (turbulent);
Re_0, Reynolds number at nozzle exit $= U_0 d_0/\nu$;
Sc_t, turbulent Schmidt number.

1. INTRODUCTION

THE PROCESS of mass transfer from saturated porous surfaces exposed to turbulent air streams finds many practical applications. In many cases, the air stream will be in the form of a wall jet over the porous surface. The aerodynamics of both

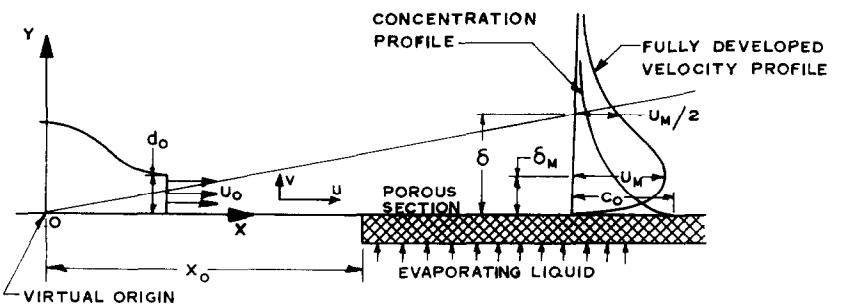

FIG. 1(a). Two-dimensional plane wall jet.